Time Reversal SWIPT Networks with an Active Eavesdropper: SER-Energy Region Analysis

Ha-Vu Tran*, Georges Kaddoum*, Hung Tran†, Duc-Dung Tran‡, and Dac-Binh Ha‡
*ETS Engineering School, University of Quebec, Montreal, Canada
Email: ha-vu.tran.1@ens.etsmtl.ca, georges.kaddoum@etsmtl.ca
†School of Innovation, Design and Engineering, Mälardalen University, Västerås, Sweden
Email: tran.hung@mdh.se
‡Faculty of Electrical and Electronics Engineering, Duy Tan University, Danang, Vietnam
Email: dung.td.1227@gmail.com, hadacbinh@duytan.edu.vn

***Abstract*—This paper analyzes a novel multiple-input single-output (MISO) simultaneous wireless information and power transfer (SWIPT) system model in the presence of an active eavesdropper over the frequency-selective fading channel. In this model, a transmitter applies the time reversal (TR) beamforming technique to combat the fading effects whereas a legitimate user employs a power splitter to jointly receive information and energy, and the active eavesdropper jams the user. Given the system model, the system performance in terms of symbol error rate (SER) and energy harvesting (EH) is analyzed. In particular, we devise a SER-energy region, instead of the conventional rate-energy region, to evaluate system performance of the SWIPT model. A moment generating function (MGF)-based method is presented to exactly derive the average SER analysis. Moreover, the closed-form expression of average *effective* harvested energy is then provided to complete SER-energy region analysis. Finally, analytical results confirmed by numerical simulations show that the TR technique can support the SWIPT system to notably improve the SER performance whereas the jamming signal can enhance the EH performance.**

***Index Terms*—SWIPT, time reversal, active eavesdropper, SER, energy harvesting, frequency-selective fading channel.**

I. Introduction

Due to the notable challenge of prolonging the lifetime of wireless devices, a trend for using simultaneous wireless information and power transfer (SWIPT) techniques is emerging [1], [2]. In this context, battery-powered devices can jointly receive information and energy from radio frequency (RF) signals sent by transmitters. Therefore, such devices are able to replenish energy via wireless environments for extending their lifetime. Most importantly, SWIPT networks have promptly found their applications in several interesting forms, e.g. wireless sensor networks, and cellular networks [1]–[3].

In view of the natural characteristics of wireless environments, the wireless information and power transfers are often subject to the multipath fading effect, a negative factor degrading the system performance and energy transfer efficiency. In this situation, beamforming techniques become a promising solution for feasible implementation of SWIPT networks. The work of [4] addresses for the first time beamforming optimization for a SWIPT system, in which the system performance is analyzed by a definition of the rate-energy region. In view of secure beamforming designs, the dual use of artificial interference and energy signals is proposed in [5] to enhance efficient energy transfer and ensure communication security. Indeed, beamforming optimization designs for SWIPT systems have been widely investigated for several wireless communication systems in various contexts [6]–[8].

Nevertheless, most of these works build their systems under the assumptions that the eavesdropper is passive and the communication channel is subject to flat fading. Our work presents two novel ideas. First, we aim to study a multiple-input single-output (MISO) time reversal (TR) SWIPT system in the presence of an active eavesdropper over frequency-selective channels. Second, we are interested in studying the SWIPT performance using a new metric region, namely the symbol error rate (SER)-energy region, instead of the conventional rate-energy region.

In our scenario, the legitimate user employs power spilitting to conduct the information decoding (ID) and energy harvesting (EH) processes, while the eavesdropper carries out a jamming action on the legitimate user. Because of the frequency-selective fading, signal power of each received symbol is not only spread out in the time domain, but also significantly leaked to unintended locations in the space domain. To deal with such issues, we propose TR beamforming technique for the SWIPT system. As a matter of fact, due to its signal focalization property, the TR technique has gained a lot of attention from the research community recently [9]–[13]. Moreover, the exact SER analysis of a MISO TR-employed system has been an interesting unsolved problem over the last few years. Although a large number of earlier research have addressed SER or BER analysis, either approximate analytical results or simulation results are provided [9], [11]–[13]. This motivates us to present a moment generating function (MGF)-based method to exactly derive the SER analysis even when the eavesdropper is jamming the legitimate user. To accomplish the EH analysis, average *effective* harvested energy metric similar to the work in [14] is proposed to evaluate the amount of average harvested energy. Accordingly, its closed-form expression is provided to complete the SER-energy region

978-1-5090-1701-0/16/$31.00 ©2016 IEEE

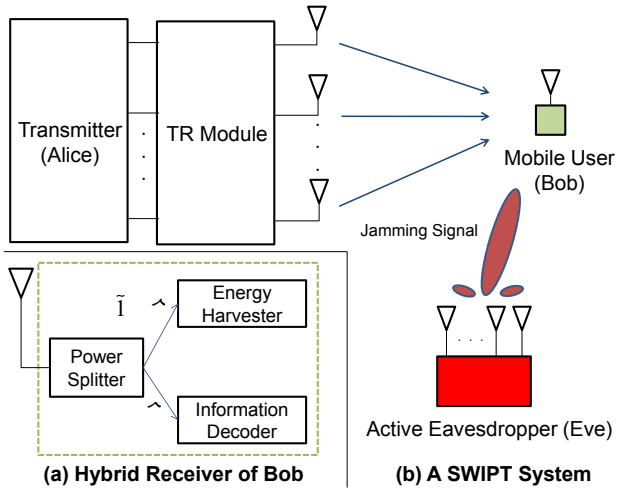

Fig. 1. a) Hybrid Receiver of Bob, b) TR SWIPT System with an Active Eavesdropper.

analysis.

The results presented in our paper show that the TR technique efficiently deals with the effects of frequency-selective fading to improve the SER performance. Moreover, the legitimate user can utilize the jamming signal from the active eavesdropper to enhance the EH performance. Finally, the validity of our analysis is verified by the use of Monte-Carlo simulation.

II. System Model

A. System model and scenario

In this paper, we consider a MISO TR SWIPT system in the presence of an active eavesdropper over frequency selective channels, as illustrated in Fig. 1. It is assumed that the transmitter (Alice) and the active eavesdropper (Eve) are equipped with M_T and M_E antennas, respectively, whereas the legitimate user (Bob) has a single antenna. Additionally, as shown in Fig. 1, Bob's hybrid receiver uses a power splitter to coordinate the processes of information decoding and energy harvesting. Assuming the channels are reciprocal, we take into account the scenario as follows

- Following TR's scheme, first, Bob initiates training phase by sending a pilot signal to Alice for estimating the channel impulse response (CIR).
- In transmission phase, Alice utilizes the time reversed version of such CIR as beamformer and then sends out the transmit signal.
- Eve aims at disrupting the reliability of Alice-Bob communication by steering the jamming signal to Bob's zone.

Given the scenario, the signals sent from Alice and Eve are captured first at Bob's power splitter and have the following discrete form

$$\mathbf{y}_B = \mathbf{y}_A + \mathbf{y}_J + \mathbf{n}_0, \tag{1}$$

where $\mathbf{y}_A$ and $\mathbf{y}_J$ are the received signal from Alice and the arrived jamming signal from Eve, respectively, and $\mathbf{n}_0$ is additive white Gaussian noise (AWGN) introduced by the splitter.

More specifically, we can write $\mathbf{y}_A$ in the following form

$$\mathbf{y}_A = \sqrt{p_A} s_A \sum_{m=1}^{M_T} \mathbf{g}_m * \mathbf{h}_m, \tag{2}$$

in which, $*$ is the convolution operator, p_A is transmit power at Alice, s_A is the transmit symbol $\left(\mathbb{E}\left[|s_A|^2\right] = 1\right)$, $\mathbf{h}_m \in \mathbb{C}^L$ is the legitimate channel between the m^{th} transmission antenna and Bob, whose taps each have a mean of $\mathbb{E}\left[h_m[l]\right] = 0$ and a variance $\mathbb{E}\left[|h_m[l]|^2\right] = \sigma^2_{m,l}$, and $\mathbf{g}_m \in \mathbb{C}^L$ is the TR beamformer which can be shown to be

$$g_m[l] = h^H_m[L+1-l] \Big/ \sqrt{\sum_{m=1}^{M_T} \|\mathbf{h}_m\|^2}. \tag{3}$$

Due to the convolution operator, $\mathbf{y}_A \in \mathbb{C}^{2L-1}$.

Moreover, the jamming signal arrived at the taps of $\mathbf{y}_J$ can be expressed as

$$\mathbf{y}_J = \begin{bmatrix} y_J[1] & y_J[2] & \dots & y_J[2L-1] \end{bmatrix}^T, \tag{4}$$

where each tap of $\mathbf{y}_J$ is assumed to be a random variable with $\mathbb{E}[y_J[l]] = 0$ and $\mathbb{E}[|y_J[l]|^2] = \sum_{n=1}^{M_E} p_{E,n}\sigma^2_{E,l}$. Note that $p_{E,n}$ is the transmit power at the n^{th} antenna of Eve, and $\sigma^2_{E,l}$ is the channel gain that the jamming signal arrives at $y_A[l]$. Furthermore, $\mathbf{n}_0 \in \mathbb{C}^{2L-1}$ and each tap $n_0[l]$ has zero mean and variance $\sigma^2_{0,l}$.

B. Signal power splitting for ID and EH

This subsection presents the signal splitting process at Bob. Using the hybrid receiver, the received signal at Bob can be divided such that a ρ portion of the received signal power is assigned to the information decoder and the rest $(1-\rho)$ portion is transferred to the energy harvester, as shown in Fig. 1.b.

First, we consider the signal processing at the information decoder. Benefiting from the power focalization property of TR, Bob only needs to take one sample at the central tap of the received signal, i.e. $\mathbf{y}_B[L]$, and to neglect the other taps. Due to Eve's attack, Alice aims at providing a highly reliable communication. In order to avoid the inter-symbol interference (ISI) in the received signal, we assume that symbol durations are less than the channel delay spread. Accordingly, the instantaneous signal-to-interference-plus-noise ratio (SINR) at the information decoder would be

$$\gamma_{\text{TR}} = \tilde{\gamma} \sum_{m=1}^{M_T} \left(g_m * h_m\right)[L], \tag{5}$$

where

$$\tilde{\gamma} = \frac{\rho p_A}{\rho\sigma^2_{E,L} + \rho\sigma^2_{0,L} + \sigma^2_{ID}} = \frac{\rho p_A}{\rho\sigma^2_{E,L} + \sigma^2_B}, \tag{6}$$

where $\sigma^2_B = \rho\sigma^2_{0,L} + \sigma^2_{ID}$, and σ^2_{ID} is the AWGN power introduced by the information decoder.

Next, we take into account the energy harvesting at Bob. The energy harvester captures the energy from the $(1-\rho)$ portion of $\mathbf{y}_A$ and $\mathbf{y}_J$. On this basis, the harvested energy at Bob can be given by

$$\psi = \xi(1-\rho)\left(p_A\left\|\sum_{m=1}^{M_T}\mathbf{g}_m * \mathbf{h}_m\right\|^2 + \|\mathbf{y}_J\|^2\right), \quad (7)$$

where $0 \leq \xi \leq 1$ is the energy conversion efficiency.

III. SER-Energy Region Analysis

In this section, the analysis of the average SER-energy region is studied. In order to characterize such region, we aim to derive the average SER and average harvested energy metrics using closed-form expressions. Such SER and harvested energy metrics are analyzed in the following subsections III. A and III. B, respectively.

A. SER analysis with MGF-based approach

In this subsection, we present a MGF-based method in order to achieve the closed-form expression of the SER at the information decoder. For initiation, since γ_{TR} is a non-negative variable, the MGF in terms of the Laplace-Stieltjes transform can be expanded to

$$\phi_{\text{TR}}(\epsilon) \triangleq \mathbb{E}\left[\exp\left(-\epsilon\tilde{\gamma}\left\|\sum_{m=1}^{M_T}(g_m * h_m)[L]\right\|^2\right)\right], \epsilon \in \mathbb{R}_+. \quad (8)$$

Since the instantaneous term in γ_{TR} can be further expressed as

$$\left\|\sum_{m=1}^{M_T}(g_m * h_m)[L]\right\|^2 = \left|\frac{\sum_{m=1}^{M_T}\sum_{l=1}^{L} h_m^*[l]h_m[l]}{\sqrt{\sum_{m=1}^{M_T}\|\mathbf{h}_m\|^2}}\right|^2 = \sum_{m=1}^{M_T}\|\mathbf{h}_m\|^2, \quad (9)$$

the MGF can be represented as follows

$$\phi_{\text{TR}}(\epsilon) = \mathbb{E}\left[\exp\left(-\epsilon\tilde{\gamma}\sum_{m=1}^{M_T}\|\mathbf{h}_m\|^2\right)\right]. \quad (10)$$

After some manipulations, the derivation of MGF is given by

$$\phi_{\text{TR}}(\epsilon) = \det\left(\mathbf{I}_{LM_T} + \epsilon\tilde{\gamma}\mathbf{\Gamma}\right)^{-1}, \quad (11)$$

where $\mathbf{\Gamma}$ is defined as

$$\mathbf{\Gamma} = \begin{bmatrix} \mathbf{\Sigma}_1 & \mathbf{0} & \dots & \mathbf{0} \\ \mathbf{0} & \mathbf{\Sigma}_2 & \dots & \mathbf{0} \\ \vdots & \vdots & \ddots & \vdots \\ \mathbf{0} & \mathbf{0} & \dots & \mathbf{\Sigma}_{M_T} \end{bmatrix}, \quad (12)$$

with

$$\mathbf{\Sigma}_m = \begin{bmatrix} \sigma_{m,1}^2 & 0 & 0 & 0 \\ 0 & \sigma_{m,2}^2 & 0 & 0 \\ 0 & 0 & \ddots & 0 \\ 0 & 0 & 0 & \sigma_{m,L}^2 \end{bmatrix}. \quad (13)$$

Especially, in the case of $\mathbf{\Sigma} = \mathbf{\Sigma}_1 = ... = \mathbf{\Sigma}_{M_T}$, the MGF can be simplified as

$$\phi_{\text{TR}}(\epsilon) = \text{tr}\left(\mathbf{I}_{LM_T} + \epsilon\tilde{\gamma}\mathbf{\Sigma}\right)^{-M_T}. \quad (14)$$

Generally, thanks to the MGF expression, the SER can be generalized for many modulation schemes, such as $\mathcal{M}$-ary phase-shift keying (PSK) and $\mathcal{M}$-ary amplitude-shift keying (ASK). As an illustration, consider $\mathcal{M}$-PSK modulation over fading channels, the SER can be shown as

$$P_e(\gamma_{\text{TR}}) = \frac{1}{\pi}\int_0^{\pi-\pi/\mathcal{M}} \exp\left(-\frac{\sin^2(\pi/\mathcal{M})\gamma_{\text{TR}}}{\sin^2\theta}\right)d\theta. \quad (15)$$

Accordingly, the average of the SER is given by

$$\bar{P}_e = \mathbb{E}[P_e(\gamma_{\text{TR}})] = \frac{1}{\pi}\int_0^{\pi-\pi/\mathcal{M}} \phi_{\text{TR}}\left(\frac{\sin^2(\pi/\mathcal{M})}{\sin^2\theta}\right)d\theta. \quad (16)$$

Based on the MGF, similar SER expressions can be derived for any modulation scheme with an arbitrary polygonal two-dimensional constellation.

B. Closed-form expression of average harvested energy

In this subsection, the EH performance at Bob is analyzed. Specifically, the average harvested energy can be computed according to (7) as follows

$$\bar{\psi} = \xi(1-\rho)\left(p\mathbb{E}\left[\left\|\sum_{m=1}^{M_T}\mathbf{g}_m * \mathbf{h}_m\right\|^2\right] + \mathbb{E}\left[\|\mathbf{y}_J\|^2\right]\right). \quad (17)$$

It is clear that

$$\mathbb{E}\left[\|\mathbf{y}_J\|^2\right] = \sum_{n=1}^{M_E} p_{E,n}\sum_{l=1}^{2L-1}\sigma_{E,l}^2, \quad (18)$$

however, the statistical average $\mathbb{E}\left[\left\|\sum_{m=1}^{M_T}\mathbf{g}_m * \mathbf{h}_m\right\|^2\right]$ is quite complex. Accounting for $\left(\sum_{m=1}^{M_T}\mathbf{g}_m * \mathbf{h}_m\right) \in \mathbb{C}^{2L-1}$, the L^{th} tap is considered as the main tap whereas the $l^{\text{th}}(l \neq L)$ tap is treated as the secondary tap. For convenience, we introduce the parameter $\bar{\mathtt{P}}_{\mathtt{tap}}(l)$ defined as

$$\bar{\mathtt{P}}_{\mathtt{tap}}(l) = \mathbb{E}\left[\left\|\sum_{m=1}^{M_T}(g_m * h_m)[l]\right\|^2\right]. \quad (19)$$

Taking into account the main tap, interestingly, one can see that through setting $\tilde{\gamma}=1$, $\bar{\mathtt{P}}_{\mathtt{tap}}[L]$ can be computed following the MGF-based approach by using the first order cumulant as

$$\begin{aligned}\bar{\mathtt{P}}_{\mathtt{tap}}[L] &= -\frac{d}{d\epsilon}\ln\phi_{\mathrm{TR}}(\epsilon)\Big|_{\epsilon=0,\tilde{\gamma}=1} \\ &= -\frac{d}{d\epsilon}\ln\det\left(\mathbf{I}_{LM_T}+\epsilon\tilde{\gamma}\mathbf{\Gamma}\right)^{-1}\Big|_{\epsilon=0,\tilde{\gamma}=1}. \end{aligned} \quad (20)$$

With the differential derivation, the closed-form derivation of $\bar{\mathtt{P}}_{\mathtt{tap}}[L]$ can be given by

$$\begin{aligned}\bar{\mathtt{P}}_{\mathtt{tap}}[L] &= \mathrm{tr}\left(\left(\mathbf{I}_{LM_T}+\epsilon\tilde{\gamma}_{\mathrm{TR}}\mathbf{\Gamma}\right)^{-1}\tilde{\gamma}_{\mathrm{TR}}\mathbf{\Gamma}\right)\Big|_{\epsilon=0,\tilde{\gamma}=1} \\ &= \mathrm{tr}\mathbf{\Gamma}. \end{aligned} \quad (21)$$

Thus, the average signal-to-noise (SNR) can be defined as

$$\mathbb{E}\left[\mathrm{SNR}\right] = p_A\bar{\mathtt{P}}_{\mathtt{tap}}[L]/\sigma_B^2. \quad (22)$$

On the other hand, the closed-form expression of the power on the l^{th} secondary tap directly relates to the formulation $\mathbb{E}\left[\frac{a}{b}\right]$ (a and b are two random variables); Thus, it is impossible to find a closed-form expression in this case. Similar to the works [10], [14], we employ an effective form $\frac{\mathbb{E}[a]}{\mathbb{E}[b]}$ to evaluate the $\bar{\mathtt{P}}_{\mathtt{tap}}(l)$. Given this context, we derive the average effective power of the l^{th} secondary tap $\hat{\mathtt{P}}_{\mathtt{tap}}(l)$ as

$$\begin{aligned}&\bar{\mathtt{P}}_{\mathtt{tap}}(l)(1\le l\le L-1) \\ &\simeq \hat{\mathtt{P}}_{\mathtt{tap}}(l) = \frac{\mathbb{E}\left[\left\|\sum_{m=1}^{M_T}\sum_{k=1}^{l}h_m^H[L+1-k]h_m[l+1-k]\right\|^2\right]}{\mathbb{E}\left[\sum_{m=1}^{M_T}\|\mathbf{h}_m\|^2\right]}, \end{aligned} \quad (23)$$

Note that $\hat{\mathtt{P}}_{\mathtt{tap}}(l)=\hat{\mathtt{P}}_{\mathtt{tap}}(2L-l)$ due to the symmetric property of the convolution operator.

According to (23), the closed-form expression of $\hat{\mathtt{P}}_{\mathtt{tap}}(l)$ can be expanded as

$$\hat{\mathtt{P}}_{\mathtt{tap}}(l) = \frac{\sum_{m=1}^{M_T}\sum_{k=1}^{l}\sigma_{m,l+1-k}^2\sigma_{m,L+1-k}^2}{\sum_{m=1}^{M_T}\sum_{l=1}^{L-1}\sigma_{m,l}^2}. \quad (24)$$

Due to space contraints, the proof of this derivation is omitted. By combining (17) and (24), we can derive that

$$\begin{aligned}&\bar{\psi}\simeq\hat{\psi}=\xi(1-\rho)\times \\ &\left(p_A\mathrm{tr}\mathbf{\Gamma}+2p_A\sum_{l=1}^{L-1}\hat{\mathtt{P}}_{\mathtt{tap}}(l)+\sum_{n=1}^{M_E}p_{E,n}\sum_{l=1}^{2L-1}\sigma_{E,l}^2\right), \end{aligned} \quad (25)$$

in which $\hat{\psi}$ denotes the average effective harvested energy.

Finally, based on the closed-form derivations of the SER and effective harvested energy, the average SER-energy region $\mathcal{C}_{\text{SER-E}}$ in the case of $\mathcal{M}$-ary PSK can be defined as

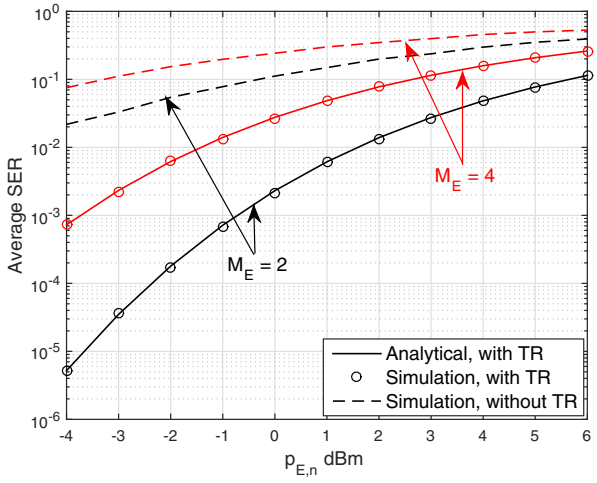

Fig. 2. SER performance. $\mathbb{E}[\mathrm{SNR}]=20$ dB (eq. (22)), $\rho=0.5$.

$$\begin{aligned}\mathcal{C}_{\text{SER-E}} \triangleq \bigcup_{0\le\rho\le1}\Bigg\{&(\bar{P}_e,\hat{\psi}):\bar{P}_e\ge\int_0^{\pi-\frac{\pi}{\mathcal{M}}}\frac{\phi_{\mathrm{TR}}\left(\frac{\sin^2(\pi/\mathcal{M})}{\sin^2\theta}\right)}{\pi}d\theta\,, \\ &\hat{\psi}\le\xi(1-\rho)\left(p_A\mathrm{tr}\mathbf{\Gamma}+2p_A\sum_{l=1}^{L-1}\hat{\mathtt{P}}_{\mathtt{tap}}(l)+\sum_{n=1}^{M_E}p_{E,n}\sum_{l=1}^{2L-1}\sigma_{E,l}^2\right)\Bigg\}. \end{aligned} \quad (26)$$

IV. Numerical Results

In this section, numerical results are shown to validate our analysis. The system parameters are set as follows: the transmit power is set to be $p_A=35$ dBm. Energy conversion efficiency ξ is chosen to be 50%. Furthermore, the 8-PSK modulation scheme is evaluated.

Considering the Alice-Bob link, we employ the wireless local area network (WLAN) channel model (model B) [15] in which 20 MHz bandwidth is used to transmit the data on a carrier frequency of 2.4 GHz. Accounting for the power of the jamming signal received at Bob (see (4)), we set $\sigma_E^2=\sigma_{E,1}^2=\ldots=\sigma_{E,2L-1}^2=1$ mW and $p_{E,1}=p_{E,2}=\ldots=p_{E,M_E}$. On the other hand, the distance from Alice to Bob is arranged to be 40 m whereas Eve is randomly located (following a uniform distribution) in a circle of radius 6 m from Bob. Moreover, the path loss exponent is set to be $\alpha=3$.

Fig. 2 indicates the SER performance variation under different transmit power levels of Eve, i.e. values of M_E. It is visible that the analytical results well match the simulation results. Furthermore, the SER increases when M_E scales up. This demonstrates the fact that the SER performance degrades when Eve increases the power of the jamming signal towards the Bob. On the other hand, considering the cases with/without the TR, one can conclude that employing the TR technique at the transmitter can help the SWIPT system significantly improve the SER performance.

From Fig. 3, one can evaluate that the results of the average *effective* harvested energy match those of the average harvested

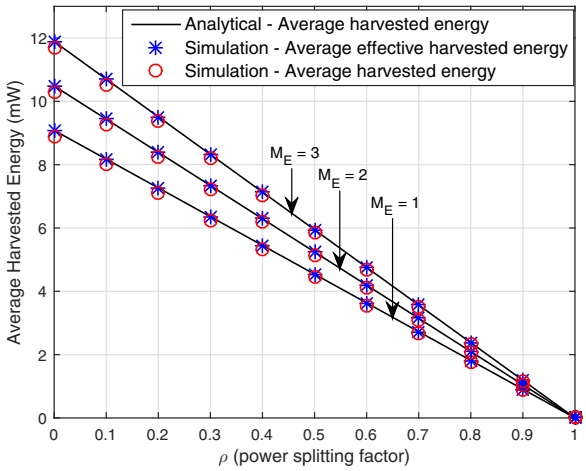

Fig. 3. EH performance.

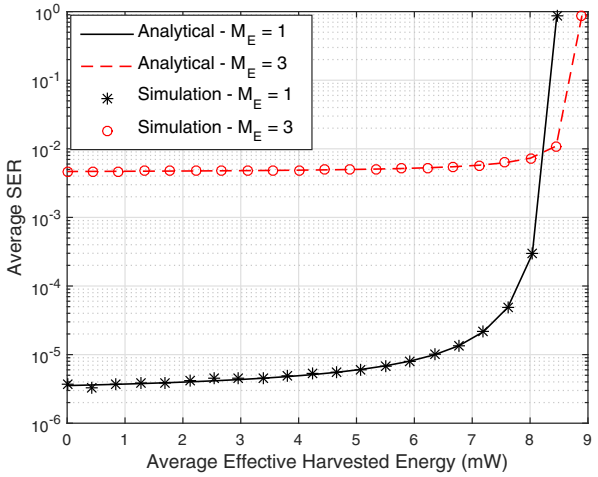

Fig. 4. SER-Energy region. $\{p_{E,n}\}_{n=1}^{M_E} = -1$ dBm.

energy very well. Indeed, these metrics have very similar characteristics; However, the average effective harvested energy metric has a much lower mathematical complexity compared to the average effective harvested energy one. Moreover, we can see that the EH performance is inversely proportional to the value of ρ. In particular, Bob's energy harvester is able to benefit from the strength of the jamming signal sent from Eve. In other words, the attack from Eve facilitates the EH performance, nevertheless, it hurts the SER performance.

Based on the analysis of the SER and EH, we investigate the SER-energy region. In Fig. 4, an illustration of the SER-energy region is shown for the TR-employed system with 8-PSK modulation and power splitting scheme. It can be observed that there exists a trade-off between the reliability of ID in terms of the SER and the performance of the EH regarding the amount of harvested energy. Generally, such achievable region can be obviously exhibited by our analysis.

V. Conclusion

In this paper, we first propose employing the TR technique to a SWIPT network in the presence of an active eavesdropper over frequency-selective fading channels. The performance of this SWIPT network is investigated by use of the proposed SER-energy region. Particularly, we present an MGF-based approach to derive the closed-form SER expression for the SWIPT system. The average effective harvested energy metric is demonstrated as a promissing replacement for the average harvested energy metric for measuring EH performance. Finally, our results indicate that the TR technique efficiently deals with frequency selective fading effects and improves the SER performance; Also, the EH performance benefits from the jamming signal of the malicious jammer.

References

[1] X. Lu, P. Wang, D. Niyato, D. I. Kim, and Z. Han, "Wireless networks with RF energy harvesting: A contemporary survey," *IEEE Comm. Surveys & Tutorials*, vol. 17, no. 2, pp. 757–789, 2015.

[2] L. Liu, R. Zhang, and K.-C. Chua, "Wireless information transfer with opportunistic energy harvesting," *IEEE Trans. Wireless Commun.*, vol. 12, no. 1, pp. 288–300, 2013.

[3] X. Lu, D. Niyato, P. Wang, D. I. Kim, and Z. Han, "Wireless charger networking for mobile devices: fundamentals, standards, and applications," *IEEE Wireless Commun. Mag.*, vol. 22, no. 2, pp. 126–135, 2015.

[4] R. Zhang and C. K. Ho, "MIMO broadcasting for simultaneous wireless information and power transfer," *IEEE Trans. Wireless Commun.*, vol. 12, no. 5, pp. 1989–2001, 2013.

[5] D. Ng, E. Lo, and R. Schober, "Robust beamforming for secure communication in systems with wireless information and power transfer," *IEEE Trans. Wireless Commun.*, vol. 13, no. 8, pp. 4599–4615, 2014.

[6] M. Khandaker and K.-K. Wong, "SWIPT in MISO multicasting systems," *IEEE Wireless Commun. Lett.*, vol. 3, no. 3, pp. 277–280, 2014.

[7] J. Xu, L. Liu, and R. Zhang, "Multiuser MISO beamforming for simultaneous wireless information and power transfer," *IEEE Trans. Signal Process.*, vol. 62, no. 18, pp. 4798–4810, 2014.

[8] H. Lee, S. Lee, K. Lee, H. Kong, and I. Lee, "Optimal beamforming designs for wireless information and power transfer in MISO interference channels," *IEEE Trans. Wireless Commun.*, vol. 14, no. 9, pp. 4810–4821, 2015.

[9] B. Wang, Y. Wu, F. Han, Y.-H. Yang, and K. Liu, "Green wireless communications: A time-reversal paradigm," *IEEE J. Sel. Areas Commun.*, vol. 29, no. 8, pp. 1698–1710, 2011.

[10] F. Han, Y.-H. Yang, B. Wang, Y. Wu, and K. Liu, "Time-reversal division multiple access over multi-path channels," *IEEE Trans. Commun.*, vol. 60, no. 7, pp. 1953–1965, 2012.

[11] T. Kaiser and F. Zheng, *Ultra-wideband Systems with MIMO*. Wiley, 2010.

[12] M. Maaz, M. Helard, P. Mary, and M. Liu, "Performance analysis of time-reversal based precoding schemes in MISO-OFDM systems," in *Proc. of the 81st IEEE Vehicular Technology Conference (VTC Spring)*, Glasgow, UK, May 2015, pp. 1–6.

[13] T. Dubois, M. Helard, M. Crussiere, and C. Germond, "Performance of time reversal precoding technique for miso-ofdm systems," *EURASIP Journal on Wireless Communications and Networking*, 2013.

[14] H.-V. Tran, H. Tran, G. Kaddoum, D.-D. Tran, and D.-B. Ha, "Effective secrecy-SINR analysis of time reversal-employed systems over correlated multi-path channel," in *Proc. of 11th IEEE International Conference on Wireless and Mobile Computing, Networking and Communications (WiMob)*, Abu Dhabi, United Arab Emirates, Oct. 2015, pp. 527–532.

[15] M. Hernandez, H.-B. Li, I. Dotlic, and R. Miura, "Channel models for tg8," IEEE, Tech. Rep., 2012. [Online]. Available: https://mentor.ieee.org/802.15/dcn/12/15-12-0459-00-0008-tg8-channel-models.doc